An Innovative Two-Source Large-Signal Measurement System for the Characterization of Low-Frequency Dispersive Effects in FETs

Antonio Raffo[1], Valeria Vadalà[1], Pier Andrea Traverso[2], Alberto Santarelli[2], Giorgio Vannini[1], Fabio Filicori[2].

[1] *Department of Engineering, University of Ferrara, Via Saragat 1, 44100 – Ferrara, Italy.*
[2] *DEIS - Department of Electronics, Computer Science and Systems, University of Bologna, Viale Risorgimento 2, 40136 – Bologna, Italy.*

Abstract- Large-signal measurement systems based on high-frequency sinusoidal excitations have been widely exploited by the microwave community for the characterization of transistors under nonlinear operation. However, device characterization at high-frequencies necessarily involves the application of rather complex calibration procedures of the measurement setup. In addition, reactive effects associated with the device extrinsic parasitic effects tend to become more important at high-frequencies. Thus, uncertainties in the identification of the parasitic network components may leads in this case to critical errors in the identification of the intrinsic device behavior and in particular, of the drain current source. In order to overcome these problems, an alternative nonlinear measurement setup based on large-signal sinusoidal excitation at low-frequency (e.g., 2 MHz) is here proposed. The description of its hardware and software implementation is dealt with in this paper and different experimental examples are provided in order to highlight the capabilities of the proposed characterization approach.

I. Introduction

Low-frequency (LF) dispersive effects due to both self-heating and the presence of deep level traps and surface state densities must be accounted for, when dealing with large-signal modeling of FETs based on III-V compound semiconductors. In fact, the accurate description of these phenomena strongly enhances the capability of obtaining accurate predictions also at millimeter-wave frequencies. This issue, sometimes neglected in the past years, has proved as extremely important in the context of empirical modeling of electron devices for microwave integrated circuit design. In particular, the large-signal behavior under LF operation can not be simply described on the basis of static I/V characteristics, since dispersive phenomena cause important deviations between the static and the LF dynamic I/V curves. It is worth noting, that a complete modeling of these phenomena would involve the description of the nonlinear device behavior in the presence of port excitations having a totally general spectral components allocation over the frequency axis. However, signal spectra in the framework of typical microwave circuit applications lay well above the upper cut-off frequency of dispersive effects (apart from the dc component). Thus, unless strong nonlinear operation is involved in the presence of complex signal excitations, device models able to describe the LF dynamics above the upper cutoff frequency of dispersive phenomena are well appropriate for circuit design.

In such a context, many efforts have been made by several research groups to take into account LF dispersion both in look-up-table based and equivalent circuit models [1]-[2]. Beside dc and small-signal measurements, many of these modeling approaches need pulsed I/V measurements during the identification phase for improved prediction accuracy. As well known, the main advantage of dynamic I/V large-signal characterization carried out through the application of very short voltage pulses consists in preserving the mean values of the junction temperature and the state variables describing the trap dynamics nearly equal to the corresponding quiescent values. Due to this feature, pulsed characterization leads to isothermal and isodynamic I/V curve sets, which can be directly assumed as a reasonable description of the "local" device behavior in the neighborhood of a particular quiescent condition.

Unfortunately, besides requiring special-purpose measurement setups [3]-[4], the application of voltage pulses also presents some drawbacks. For example, a critical point is related to the extremely wide spread of the pulsed-waveform spectral components. In fact, bias-dependent frequency behavior of device-under-test (DUT) input and output impedances, bandwidth limitation of cables, bias networks and other components of the measurement setup, may actually "extend" the real duration of pulses in such an almost unpredictable way. This leads to critical calibration procedures and possibly sub-optimal choices of the sampling times for current acquisitions [5]. Thus, the achievable measurement accuracy is often rather limited and not always easily evaluated.

Finally, it is worth noting that pulsed I/V operation is strongly different from actual operating conditions of an electron device used in typical microwave circuits, where a large-signal sinusoidal or distorted sinusoidal regime is instead very common.

An alternative large-signal I/V measurement system is here presented, where the DUT is simply excited through two LF sinusoidal voltage sources. The new measurement setup is described in Section II both in its hardware and software details, while typical experimental results are presented in Section III.

II. The proposed two-source large-signal measurement system

In order to characterize the nonlinear electron device performance, different measurement systems have been proposed [6-8]. In most of these setups the device is forced to work under sinusoidal or, more generally, distorted sinusoidal regime, which is very common in microwave applications (e.g., Power Amplifier). On the other hand, when the characterization is oriented to LF phenomena, the pulsed regime is sometime preferred to the sinusoidal one. The proposed system allows to apply low-frequency large-signal sinusoidal excitations at both ports of an electron device. It can be considered as an extension of [9], although capabilities and flexibility are by far extended in this setup. The measurement procedure limitations of the original system, related to the single port excitation and the choice of a resistive loading condition, are here overcame by adopting two sources with active load synthesis capabilities. The implementation of an arbitrary loading condition is essential to quickly characterize the DUT under very different operating conditions. A complete characterization of the device is obtainable with this instrumentation, by involving any operation of interest and by measuring dynamic current/voltage (I/V) loci at the device ports.

A. The setup architecture

The measurement system proposed is shown in Fig. 1. An arbitrary function generator (having 50 ohm input impedance) with two independent channels, is used to feed the DUT with two sinusoidal waveforms at low-frequency (e.g., a few MHz). The operating frequency is chosen in order to characterize the device behavior above the upper cut-off frequency (f_{co}) associated with dispersive phenomena (typically some hundreds of kilohertz). A four-channels sampling oscilloscope (1 GSa/s) provides acquisition of the DUT incident and reflected waves; an impedance of 50 ohm is selected at each input channel. Monitoring of incident and reflected waves at the DUT input and output ports is obtained by means of two wide-bandwidth (10 kHz – 1000 MHz) dual directional couplers, while two 100 kHz–6000 MHz bandwidth bias-tees with low-insertion loss (0.15 dB) provide both dc and rf path isolation and device stability. The dc source applies the bias and measures the average values of the electrical variables at the device ports. A microwave probe station is needed for on-wafer measurements.

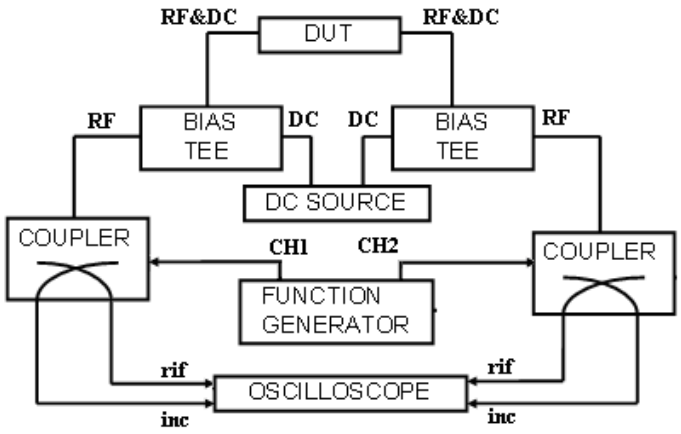

Figure 1. The proposed large-signal measurement setup.

At the frequency of a few megahertz all the measurement system components satisfy linear non-distortion conditions, greatly simplifying the calibration procedure required for the reconstruction of the dynamic I\V loci at the device ports. To this aim, the setup can be divided into six signal paths to be characterized in terms of attenuation and delay in the operating frequency range (i.e., [2 MHz – 16 MHz]): a) from channel 1 of signal generator section to DUT input port; b) from channel 1 of signal generator section to oscilloscope section (input port incident wave acquisition section); c) from DUT input port section to oscilloscope section (input port reflected wave acquisition section); d) from channel 2 of signal generator section to DUT output-port; e) from channel 2 of signal generator section to oscilloscope section (output port incident wave acquisition section); f) from DUT output port section to oscilloscope section (output port reflected wave acquisition section). Table I shows the characterization data for each path, i.e. the average values over the operating frequency range of the attenuation and delay of each signal path:

Path	a	b	c	d	e	f
Delay [ns]	10.9	8.35	10.2	10.8	8.2	10.3
Attenuation [dB]	0.3	40.0	40.1	0.4	40.1	40.1

Tab. I. Characterization of elementary signal-paths of the measurement setup averaged over the operating frequency range.

Once the characterization procedure has been carried out, a coherent linear model of the measurement system can be easily implemented into a commercial CAD environment oriented to microwave circuit design (e.g., Agilent Advanced Design System), as shown in Fig. 2.

The validity of the calibration procedure has been tested by replacing the DUT with two isolated 12.5 ohm resistances connected at the input and the output ports. The selected resistances make part of an alumina calibration substrate and

are designed to properly work up to 110 GHz. These two terminations are therefore purely resistive at few megahertz. The incident and reflected waveforms were measured under sinusoidal excitation at different frequencies and the reconstructed current\voltage (I\V) loci were compared with the corresponding simulated results. Output current loci at selected frequencies within the operating range are shown in Fig. 3. Measurements and simulations are here compared both at the oscilloscope section and at the device port. As it can be noted, perfect instrument calibration is achieved. Identical results were obtained at the input port.

B. The controlling software

The measurement setup is fully controlled via an IEEE488 standard interface by means of a commercial instrument automation software running on a PC (e.g., NI LabVIEW). The developed control-software allows the user to make data acquisitions under nonlinear dynamic regime by controlling all the instruments in the system. The developed graphical user interface (GUI) is shown in Fig. 4: both dc-parameters, such as bias values and corresponding compliances, and ac-parameters, such as amplitudes and relative phase of the generated signals, are easily defined by means of the GUI. The controlling program enables acquisitions in two measurement-modes, which will be referred to in the following as "*scatter-mode*" and "*sweep-mode*".

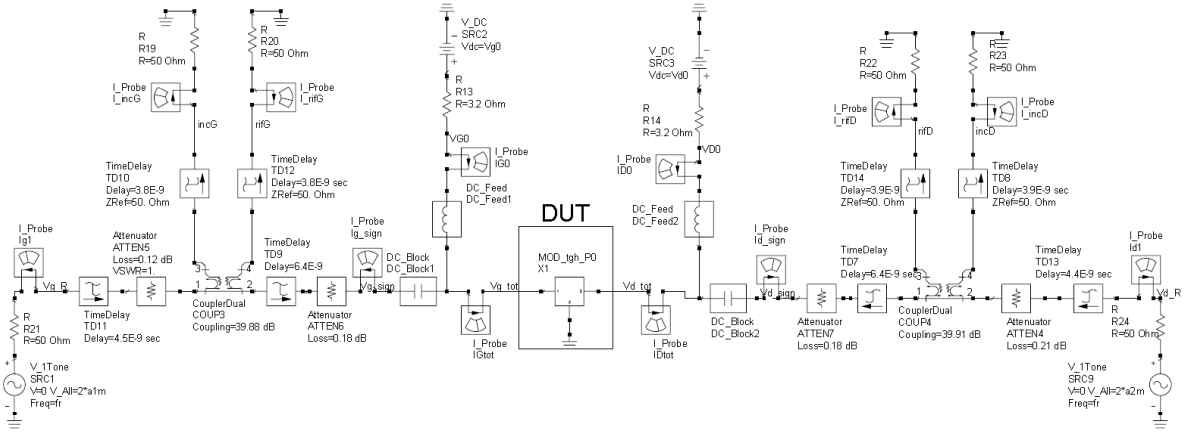

Figure 2. Model of the proposed measurement system implemented into a commercial CAD tool.

In the scatter-mode, the user manually defines the desired sequences of dc- and ac-parameters to be used for bias and signal generation. This is very useful when just a few measurements are needed, as when a preliminary device performance evaluation has to be carried out. Alternatively, in the sweep-mode, the program asks the user for grids of: dc bias points, signal amplitudes and relative phases (dc and ac sections are labeled as "A" and "B", respectively, in Fig. 4). This operation mode is essential for an extensive characterization of device dispersive phenomena, since it allows to carry out measurements in a systematic way, by sequentially adopting bias points on a selected grid and by sweeping amplitudes and phases of input and output signals according to arbitrarily complex schemes.
Experimental data at the DUT ports are shown in Fig. 5 for a 0.25-µm GaAs PHEMT. The advantages of the sweep-mode are here clearly put in evidence. For example, measurements shown in Fig. 5a were carried out by maintaining constant bias conditions (class-A device operation: V_{g0} = -0.6 V, V_{d0} = 5 V) and constant amplitudes of the incident signals (A_g = 0.1 V, A_d = 2 V), while their relative phase were swept over the range $0° \leq \Delta\varphi \leq 300°$ (step 60°). Another example is shown in Fig. 5b. In this case, measurements were carried out by maintaining constant bias conditions (the same class-A operation), constant relative phase of the incident signals ($\Delta\varphi$ = 180 °), constant amplitude of the drain incident signal (A_d = 2 V), while the amplitude of the gate incident signal was swept over the range $0.1 \text{ V} \leq A_g \leq 0.5$ V (step 0.1 V).

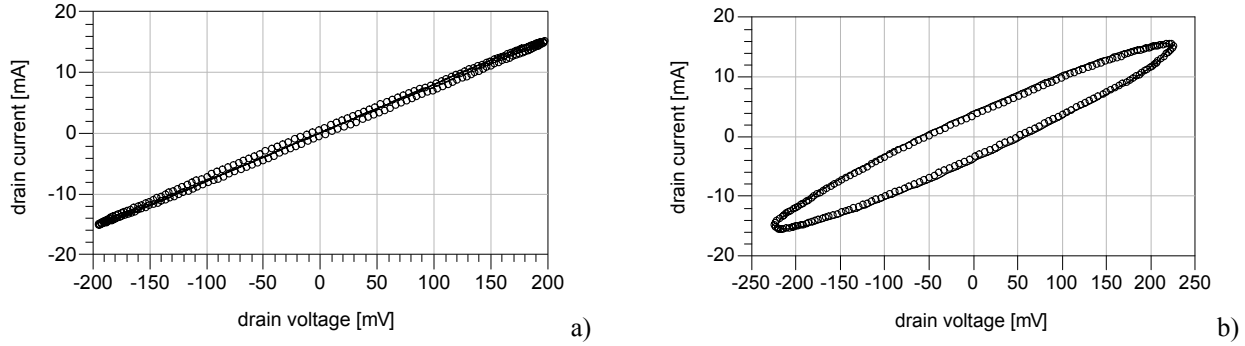

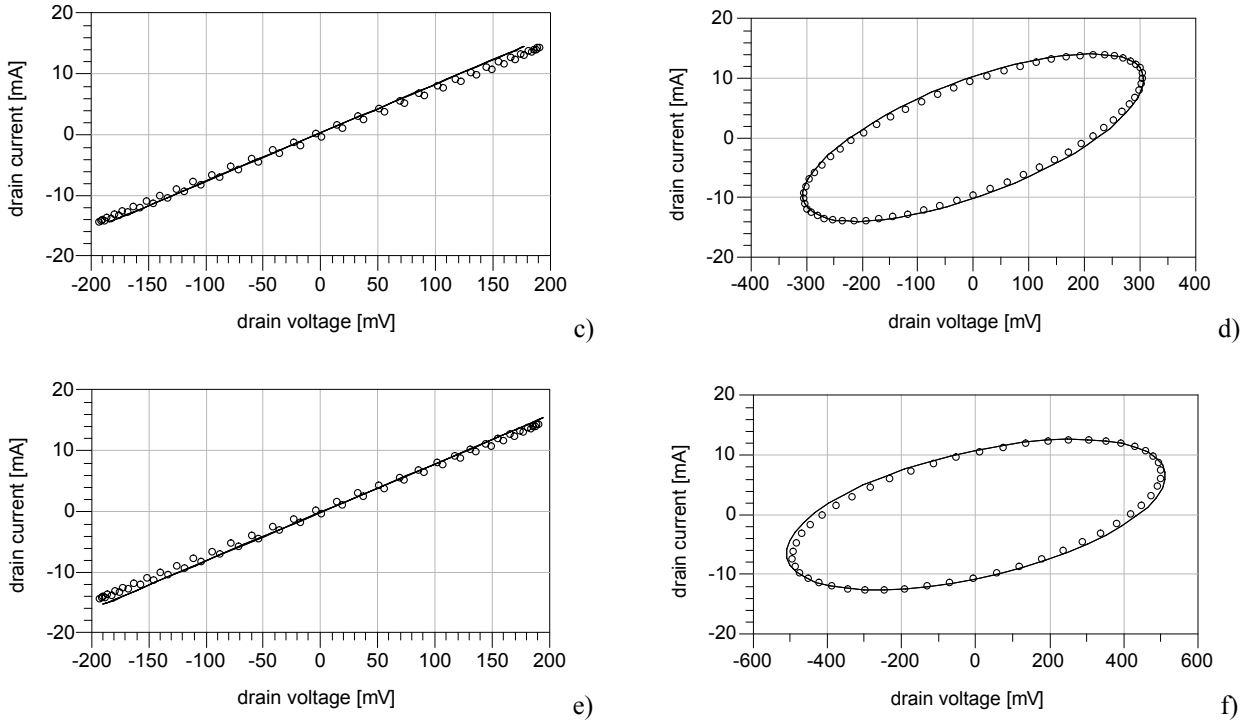

Figure 3. I\V loci at the oscilloscope (a-c-e) and device (b-d-f) sections. Comparison between measures (circles) and simulations (continuous lines). Frequency of excitations: 2 MHz (a-b), 8 MHz (c-d) and 16 MHz (e-f).

Figure 4. Main input panel of the developed Graphical User Interface and controlling software, by using the NI LabVIEW environment.

III. Experimental Results

As a practical application example of the proposed measurement setup, the dispersion effects associated with two different technological processes are compared. To this aim, different I/V loci are presented in Fig. 6-7 in the cases of two devices, a GaAs-based PHEMT (total periphery: 600 µm) and a GaN-based PHEMT (total periphery: 800 µm), respectively. The presented loci (four for each device), correspond to very different operating conditions, i.e. to

different bias and\or signals applied at the device ports. The measured I/V loci are compared in Fig.6-7 to theoretical simulation results obtained by describing the low-frequency behavior of each device through the purely static I/V characteristics (plotted as background in each figure). As it can be noted, deviations between measured and predicted current loci are minor in the case of the GaAs-based device than in the other case. Since these deviations may be somehow correlated to the assessment of the corresponding technological processes (minor deviations observed, the more assessed the process), figures 6-7 give clear indications about the relatively young GaN-based technology.
According to the highlighted features, acquisitions of dynamic I/V loci through the proposed instrumentation is believed to prove as extremely helpful in the development of accurate nonlinear models taking into account the complex low-frequency dynamics of III-V-based transistors.

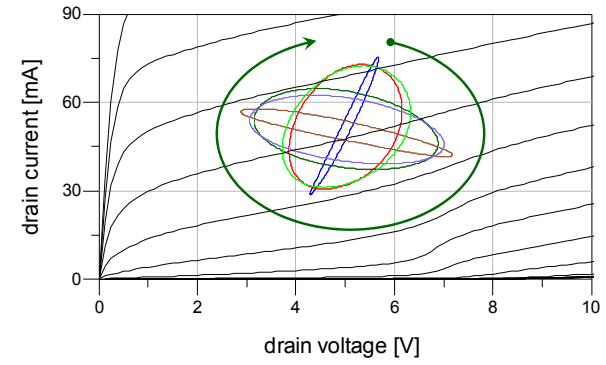

a)

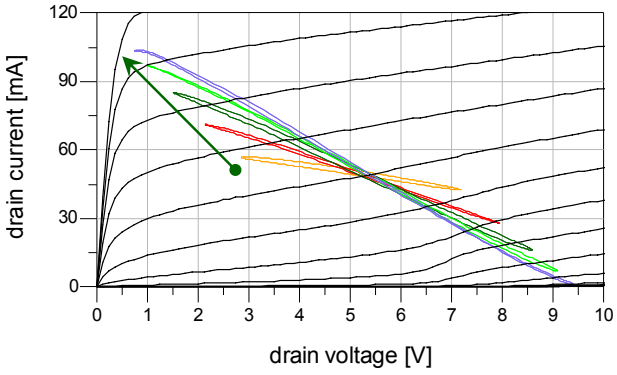

b)

Figure 5. I\V loci at the DUT sections obtained through the measurement setup operated in the sweep-mode (see text). Example a): bias conditions and amplitudes of the incident signals kept constant, relative phase swept. Example b): bias conditions, relative phase of the incident signals and amplitude of the drain incident signal kept constant, amplitude of the gate incident signal swept.

IV. Conclusions

In this paper an innovative measurement system has been presented, which allows to easily characterize LF dispersive effects well present in III-V compound semiconductor devices. In particular, the hardware and software system implementation has been widely described. Finally, different measurements carried out on PHEMT devices built according to different technological processes (GaAs- and GaN-based, respectively) have been presented in order to outline the potential capabilities of the proposed setup for the development of accurate nonlinear device models to be used in circuit design.

References

[1] A. Raffo, et al., “Accurate PHEMT Nonlinear Modeling in the Presence of Low-Frequency Dispersive Effects”, *IEEE Trans. On Microwave Theory and Techniques*, Nov. 2005, vol.53, pp. 3449-3459.

[2] W. Struble, S.L.G. Chu, M.J. Schindler, Y. Tajima, J. Huang, ”Modeling intermodulation distortion in GaAs MESFETs using pulsed I-V characteristics”, *Proc. GaAs IC Symposium*, pp. 179 - 182, Oct. 1991.

[3] A.E. Parker and D.E.Root, Pulse measurements quantify dispersion in pHEMT's, *Proc. URSI/IEEE Electron Symp Sign Syst*, 444-449, Oct. 1998.

[4] J.B. Scott, J.G. Rathmell, A.E. Parker, and M. Sayed, Pulsed device measurements and applications, *IEEE Trans Microwave Theory and Techn*, vol. 44, pp. 2718-2723, Dec. 1996.

[5] V. Camarchia, et al., “Fabrication and nonlinear characterization of GaN HEMTs on SiC and sapphire for high-power applications”, *Int. Journal of RF and Microwave CAE*, Vol. 16, pp. 70 – 80, 2006.

[6] Jan Verspecht, "Large-signal network analysis" *IEEE Microwave Magazine*, vol.6, pp 82 – 92, 2005.
[7] D. Schreurs, et al., "Straightforward and accurate nonlinear device model parameter-estimation method based on vectorial large-signal measurements", *IEEE Transactions on Microwave Theory and Techniques,* vol. 50, pp. 2315 – 2319, 2002.
[8] V. Teppati, A. Ferrero, D. Parena, U. Pisani, "Accuracy Improvement of Real-Time Load-Pull Measurements", *IEEE Transactions on Microwave Theory and Techniques,* vol. 56, pp. 610 – 613, 2007.
[9] A. Raffo, et al., "Accurate Modelling of Electron Device I/V Characteristics Through a Simplified Large-Signal Measurement Setup", *Int. Journal of RF and Microwave CAE*, Vol. 15, pp. 441-452, 2005.

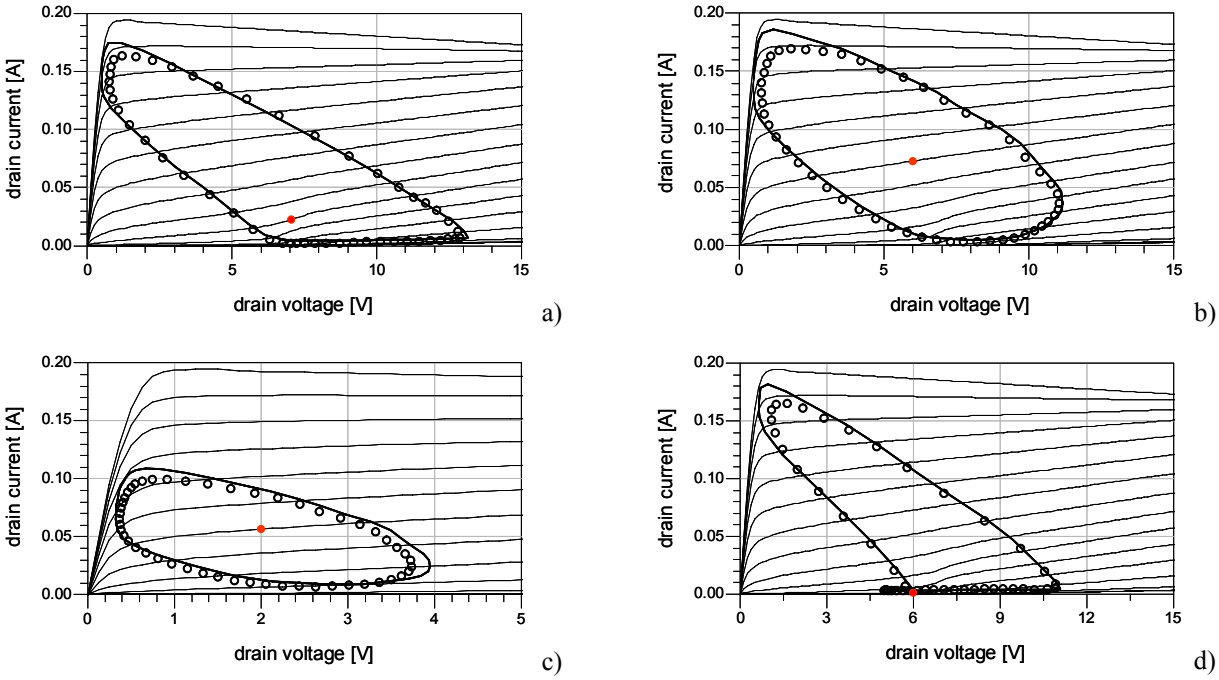

Figure 6. Dynamic I/V loci of a GaAs PHEMT. Measurements (circles) vs. model predictions based on purely-static I/V characteristics (continuous lines). Dc characteristics plotted in the background.
a) - (V_{g0} = -0.9 V, V_{d0} = 7 V, A_g = 0.9 V, A_d = 4 V, Δφ = 110°), b) - (V_{g0} = -0.6 V, V_{d0} = 6 V, A_g = 0.6 V, A_d = 4 V, Δφ = 270°), c) - (V_{g0} = -0.6 V, V_{d0} = 2 V, A_g = 0.3 V, A_d = 2 V, Δφ = 300°), and d) - (V_{g0} = -1.5 V, V_{d0} = 6 V, A_g = 1.5 V, A_d = 4 V, Δφ = 300°).

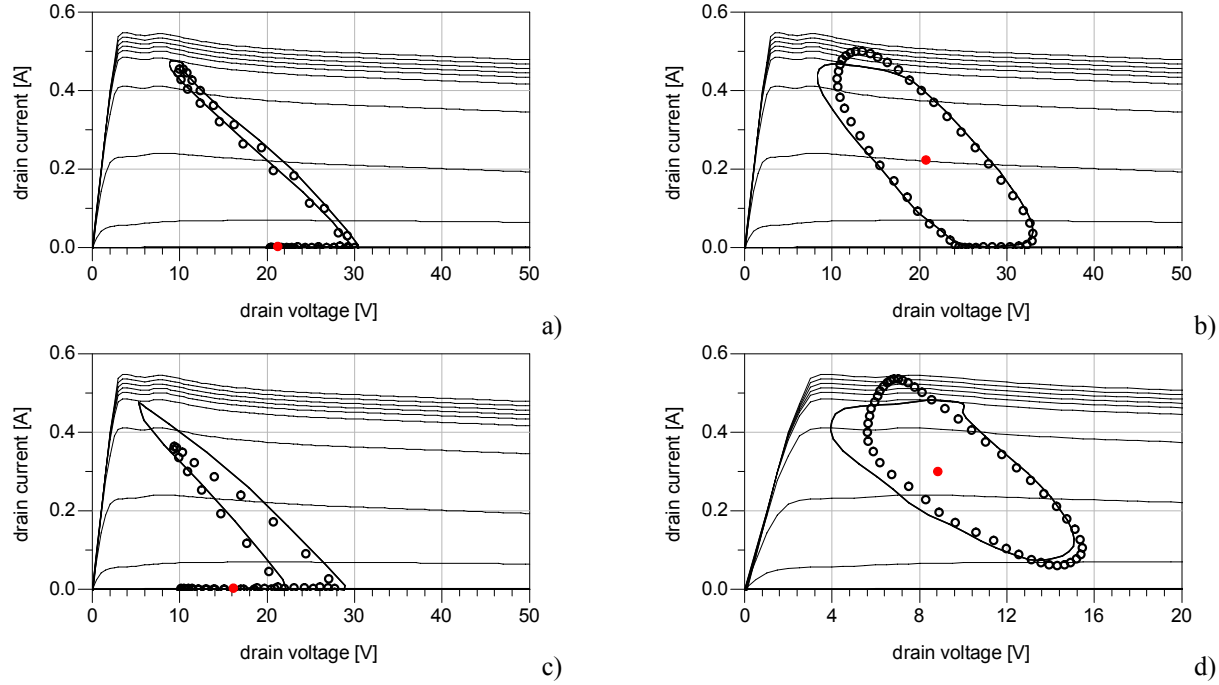

Figure 7. Dynamic I/V loci of a GaN HEMT. Measurements (circles) vs. model predictions based on purely-static I/V characteristics (continuous lines). Dc characteristics plotted in the background.
a) - (V_{g0} = -5 V, V_{d0} = 21 V, A_g = 5 V, A_d = 7 V, Δφ = 30°), b) - (V_{g0} = -2 V, V_{d0} = 21 V, A_g = 2 V, A_d = 9 V, Δφ = 60°), c) - (V_{g0} = -7 V, V_{d0} = 16 V, A_g = 7 V, A_d = 10 V, Δφ = 30°), and d) - (V_{g0} = -1.5 V, V_{d0} = 10 V, A_g = 1.5 V, A_d = 9 V, Δφ = 30°).